Search-Based vs. Task-Based Space Surveillance for Ground-Based Telescopes

Fred D. Hertwig
Air Force Institute of Technology (AFIT), Wright Patterson AFB Ohio
John M. Colombi
AFIT, Wright Patterson AFB Ohio
Richard G. Cobb
AFIT, Wright Patterson AFB Ohio
David W. Meyer
AFIT, Wright Patterson AFB Ohio

Abstract

Persistent Space Situational Awareness (SSA) is one of the top priorities of the Department of Defense (DoD). The goal of this research was to compare task-based space surveillance performance with a search-based method of space surveillance in the Geosynchronous Orbit (GEO) belt region. The performance of a ground telescope network, was modeled and simulated using Analytical Graphics Inc. (AGI's) Systems Tool Kit (STK) and Python. The model compared search-based and task-based space surveillance methods by simulating 813 Resident Space Objects (RSOs) on the summer solstice, fall equinox, and winter solstice. Four performance metrics for comparing the search-based and task-based methods were minimum detectable size, detection rate, coverage area, and latency. The search-based method modeled six different search patterns at varying starting positions. Results show that the minimum detectable size average for task-based was 47.6 cm in diameter while search-based methods ranged from 38.3–45.4 cm in diameter. Detection rate for task-based was 100% while the search-based ranged from 91.7–96.8%. Coverage area for task-based was 46% of the GEO belt and the search-based method ranged from 3.5–84.4%. Average latency (revisit time) for task-based was 78 minutes and search-based methods ranged from 62–469 minutes. It was found that task-based surveillance was the better method for current operational conditions by using a weighted decision criteria. However, as the number of RSOs increase, there is a point at which the search method has better performance.

Introduction

GEO is defined as an orbit at an altitude of about 35,780 km and the same 24-hour period as the Earth's rotation. The orbit region allows for a constant line of sight and coverage of roughly one-third of the earth with a single satellite, which is key for worldwide communication, surveillance, tracking large weather patterns, and missile warning [1]. The US Space Surveillance Network (SSN) must be able to detect space debris that could potentially cause a collision and damage or destroy operational satellites.

In task-based surveillance, a list of unique taskings are sent to each surveillance site from the Combined Space Operations Center (CSpOC).[1] The site then performs those taskings by taking images or observations of individual objects in space. The observations are then returned to the CSpOC. Images are only taken from the task list received by the site. The tasked-based process of tracking satellites leaves portions of the GEO belt unviewed for long periods of time or never viewed at all. Small area searches do occur when the expected object is not in the first field-of-view (FOV).[2] However, only a few observations are taken around where the object is expected to be in its orbit.. Nightly surveying or searching of the GEO belt could increase the probability of detection of enemy movements and orbiting space debris. In search-based space surveillance, the site would image the entire viewable sky each night and not be limited to the predetermined tasks sent by the CSpOC.

The purpose of this research is to investigate how switching to a 100% search-based space surveillance approach would affect space surveillance performance when compared with the current task-based approach. Adding new surveillance assets like ground telescopes and observation satellites would certainly increase performance of the SSN but may not be cost effective. Possible low-cost benefits could be found by simply

[1] The Joint Space Operations Center (JSpOC) transitioned to the CSpOC in July 2018.
[2] FOV is the area of the sky that the telescope can observe with one exposure.

Copyright © 2019 Advanced Maui Optical and Space Surveillance Technologies Conference (AMOS) – www.amostech.com

changing the way GEO observations are accomplished. Answering these specific research questions could provide a possible solution.

1. How does switching from tasked-based to search-based space surveillance affect GEO Space Situational Awareness (SSA) performance for a simulated ground-based telescope network?

2. How do different search patterns and constraints affect performance?

The CSpOC measures ground telescope system performance by the rate of successfully acquired tasked tracks and has in the past used tasking response time. However, to compare task-based and search-based methods, additional metrics will be used. For this research, latency acts as a surrogate for response time, and detection rate is a surrogate for the rate of successfully acquired tasked tracks. In addition, minimum detectable size and coverage area are derived and used to compare the task-based and search-based methods.

This research focused on modeling a ground-based telescope network with s a set of three sites with three telescopes each. One site is located on White Sands Missile Range near Socorro, New Mexico, one site is on Mount Haleakala, Maui, Hawaii, and one site is on the island of Diego Garcia. The model developed herein only includes the GEO belt region when evaluating the performance for the current task-based space surveillance and the proposed survey/search-based space surveillance. The model architecture will only include typical 1-meter ground telescopes and 813 known objects in the GEO belt (retrieved from spacetrack.org in 2016). The performance evaluation results for the scenario studied are assumed to be representative of how the two approaches would perform under realistic conditions.

Background

JP 3-14, Space Operations, defines SSA as "the requisite current and predictive knowledge of the space environment and the operational environment upon which space operations depend as well as all factors, activities, and events of friendly and adversary space forces across the spectrum of conflict" [1]. In other words, the US needs to know where every object in space is at all times, whether it is a friend, enemy, or piece of debris. SSA is Space Battle Management similar to that of the air domain but instead of controlling air traffic, space traffic is monitored and controlled. Having good SSA is the first step in successful and safe operations in space. General John Hyten, Commander of US Strategic Command, said in a 22 June 2018 House Armed Services Committee hearing, "As the commander responsible for defending the nation in that domain, I have to look at [Russian and Chinese] capabilities as real threats and that means I have to develop counters to those threats, which is why the first thing I have to have, just like in any other domain, is that exquisite situational awareness of what is happening in that domain so that I can respond quickly enough" [2].

The Russian satellite Olymp is an example of a possible threat that is increasing in space. Olymp was launched in September of 2014. Seven months later, it maneuvered to a spot between Intelsat 7 and Intelsat 901, which are located a half degree of longitude from each other in GEO. A few months later, it maneuvered again and settled next to another Intelsat, this time only a tenth of a degree away [3]. The US is concerned that these types of potential threats in space are on the rise. The US Intelligence Community Worldwide Threat Assessment states, "Of particular concern, Russia and China continue to launch 'experimental' satellites that conduct sophisticated on-orbit activities, at least some of which are intended to advance counterspace capabilities. Some technologies with peaceful applications—such as satellite inspection, refueling, and repair can also be used against adversary spacecraft" [4]. To be able to detect the increasing number of maneuvering satellites, the US needs to improve its SSA, whether it be through increasing the number of sensors or changing the method of how SSA is accomplished. Although detecting all satellite movements is a growing concern, it is not the only threat to space operations that is on the rise.

SSA is getting more difficult every year due to the increasing number of new satellites being launched. There has been roughly a 90% increase in the number of satellites in Low Earth Orbit (LEO) since 2014, with a current estimate of around 2,270, and the growth is expected to continue. Two private civilian companies alone have plans to launch satellite constellations that together will put upwards of 14,000 new satellites in orbit by the mid-2020s [5]. Specifically, in the GEO orbit, the increase in satellites is also occurring at a high rate. From 2000 to 2009, the number of spacecraft added to the GEO orbit exceeded the number being removed at a rate of two to one. Removal of spacecraft from the GEO orbit after the end of a mission life has been recommended for decades, but the number of large objects in GEO continues to grow [6]. According to spacetrack.org, there are currently 851 Two Line Element Sets (TLES) for known objects in the GEO belt that have received an update within the past 30 days, as of 24 July 2018. In addition to the increasing number of new satellites being launched, the amount of space debris is

Copyright © 2019 Advanced Maui Optical and Space Surveillance Technologies Conference (AMOS) – www.amostech.com

also increasing in the GEO belt. NASA estimates that there are approximately 3,250 GEO objects 10 cm or larger, as shown in Fig. 1, derived from NASA Space Debris Quarterly. The uncatalogued debris population near GEO exceeds that of the known satellite population [6]. The US Air Force created and maintains the satellite catalog that contains over 23,000 man-made earth-orbiting objects, also known as Resident Space Objects (RSOs). The satellite catalog is a database that contains the most up-to-date orbital parameters of tracked objects in space. Maintaining this catalog for the ever growing RSO population has become more difficult over the years for the SSN.

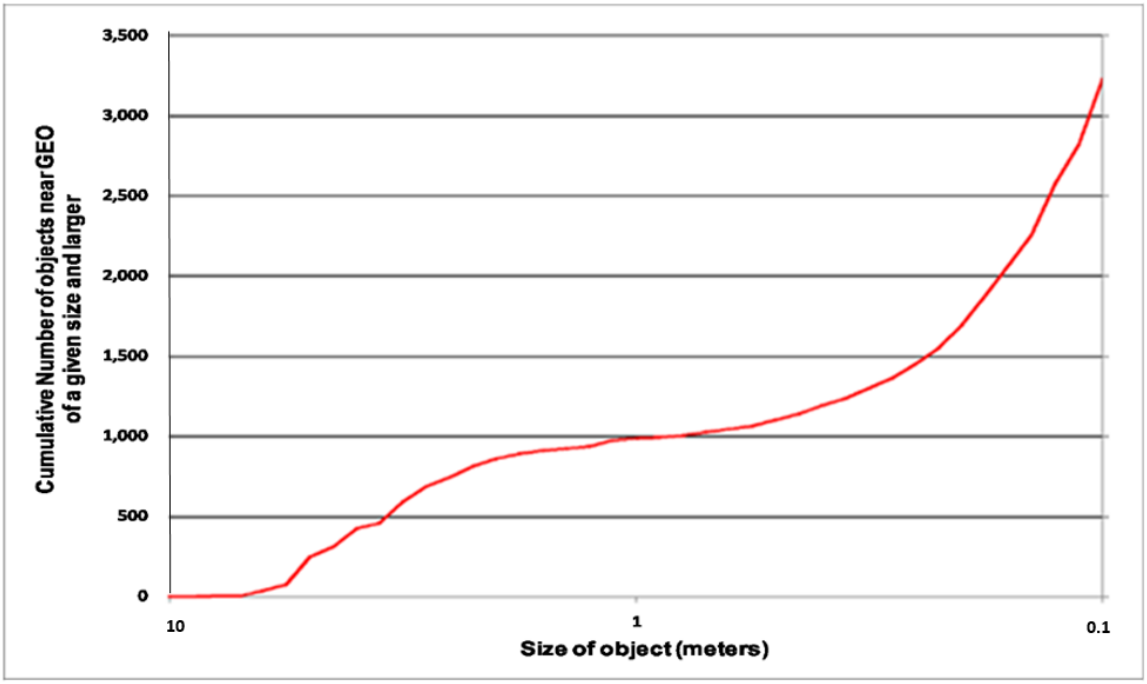

Fig. 1. NASA Assessment of the Near-GEO Satellite Population [6]

Some research has been done showing there is a need for using search-based space surveillance techniques. In the *Journal of Astronomy and Space Science*, the authors concluded, "A strategy is needed for a regional survey of geosynchronous orbits (GSOs) to monitor known space objects and detect uncatalogued space objects" [7]. STK and TLES from the CSpOC were used to simulate the orbits of 287 RSOs in view of a telescope site located in Daejoeon, South Korea. The study simulated four survey observation strategies; 5-second exposures with the 1º x 1º FOV, 5-second exposures with 2º x 2º FOV, 2-second exposures with a 1º x 1º FOV, and 2-second exposures with a 2º x 2º FOV. A scanning motion in the local reference frame was used to look at the GEO belt region that is viewable from the Daejoeon site. Fig. 2 shows the graph of a sample scan pattern used with a 2º x 2º FOV. The scan first moves vertically in the elevation direction then moves over to the next column of elevation going 17 intervals deep. Intervals are simply the width/height of the FOV used as indicated by the green and blue boxes in Fig. 2. Green indicates a 17 interval 2º x 2º FOV scan, while the blue is a single 2º x 2º FOV scan. The study found the FOV was the most important variable in obtaining high detection rates. The 5-second exposures with the 2º x 2º FOV showed the best results with detection rates of 90% and 95% for non-operational and operational RSOs respectively. A smaller observation duration increased detection rates by only 2–3%, but the longer exposure allowed for better Signal to Noise Ratio (SNR), therefore the longer exposure was chosen [7].

Copyright © 2019 Advanced Maui Optical and Space Surveillance Technologies Conference (AMOS) – www.amostech.com

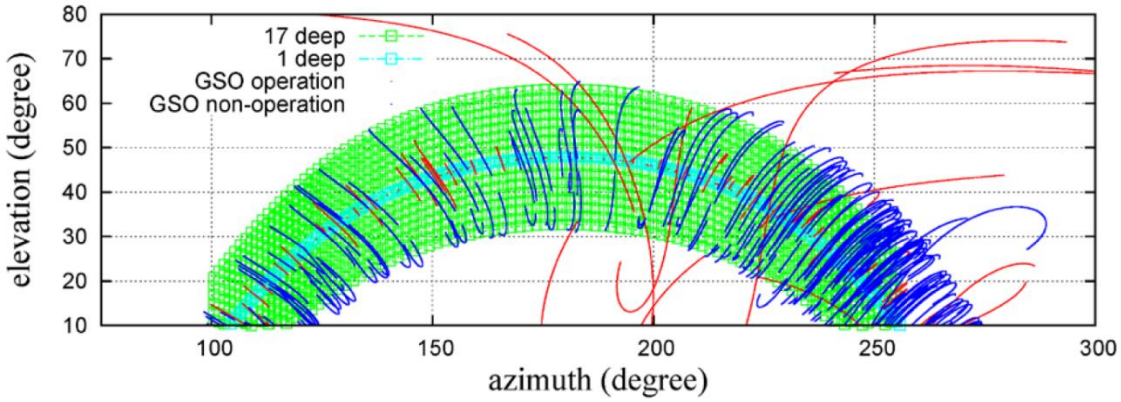

Fig. 2. Scan Pattern of the Analysis of Simulated Optical GSO Survey Observation Paper (Jin Choi 2015)

A similar study was on a possible space surveillance telescope network for the European Space Agency that was modeled to assess performance against needed requirements [8]. The model was made up of 4 telescope stations placed around the world and a catalog of 793 objects in GEO were used in the simulation. The model assumed a "stripe scan" survey strategy that picked a right ascension to follow for 24 hours and covered a declination of +/- 17º, as shown in Fig. 3. Using this scan strategy, every object with an inclination less than 17º will pass through the FOV in a 24-hour period. Due to the limited FOV of the simulated telescope, the scan will complete a full "strip" once every 15 days. The Program for Radar and Optical Observation Forecasting (PROOF) [9] tool was used to estimate the minimum detectable size and coverage. With a 1 meter telescope in survey mode, objects could be seen down to 25 centimeters in diameter and detection rates were 89.8% and 94.7% for 8-hour and 12-hour observations per night respectively. The authors concluded that a space surveillance system for GEO needs to have three to four sites and each site must be able have both dedicated survey and dedicated tasking telescopes [8].

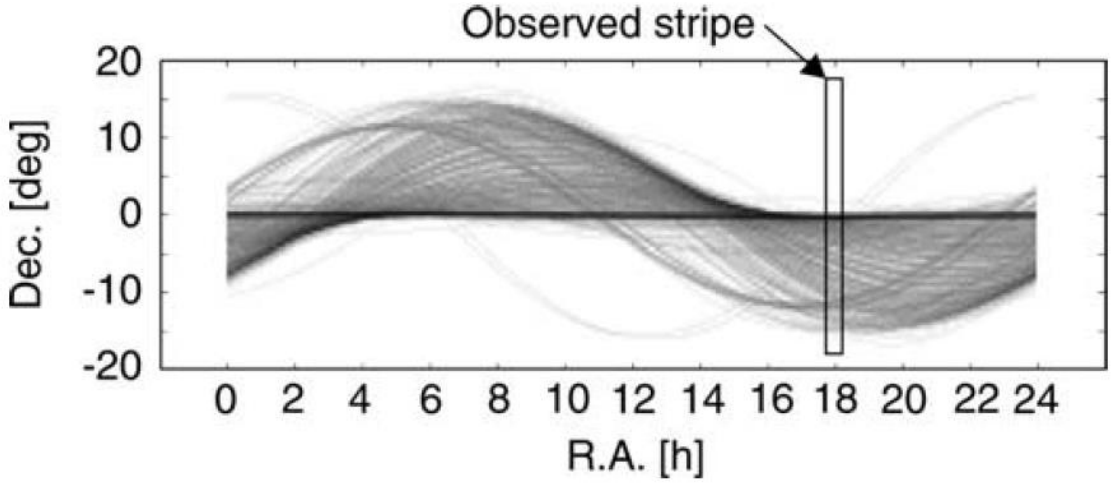

Fig. 3. Scan Pattern for Performance Estimation for GEO Space Surveillance Article [8]

Similarly, the work by Flohrer, Schildknecht, & Musci in *Advances in Space Research* states, "It is most advisable to combine survey and tasking strategy" and " 'survey only' strategy may not always be used for GEO space surveillance due to the FOV limitations. The correct detection of maneuvers cannot be guaranteed" [10]. The authors confirm that GEO should be covered by the same "stripe-scanning" approach as the 2005 "Performance estimation for GEO space surveillance" paper. The study also confirmed Choi's conclusion on wider FOVs, stating that "a wide FOV survey sensor, which covers the entire survey band, would likely be the most efficient strategy" [10].

Although previous research and implemented surveys show that there are some possible techniques for surveying and interesting trends in distributions of satellites in GEO, they do not go much beyond those results. The

Copyright © 2019 Advanced Maui Optical and Space Surveillance Technologies Conference (AMOS) – www.amostech.com

previous research and surveys do not show a good side-by-side comparison of search-based vs. task-based space surveillance. Thus, research needs to be conducted that utilizes a survey strategy for orbit maintenance and a way to compare it to the current task-based approach.

Methodology

In order to compare the task-based vs. search-based surveillance techniques, the four performance metrics (smallest detectable size, latency, detection rate, and coverage area) must be determined for each. The data generation and scheduler code used in the Stern and Wachtel (2017) thesis is used to model the baseline task-based technique while the search scheduler is newly developed. The task-based and search-based schedulers then feed into the evaluator that outputs metric values. The evaluator uses the Stern and Wachtel (2017) code to calculate the latency metric values. New code was developed to model and calculate the smallest detectable size, coverage area, and detection rate metrics for the task and search methods. Fig. 4 is a block definition diagram (BDD) that describes the items that make up the modeled ground-based GEO surveillance system. Fig. 5 is an activity diagram describing the control flow within the model created.

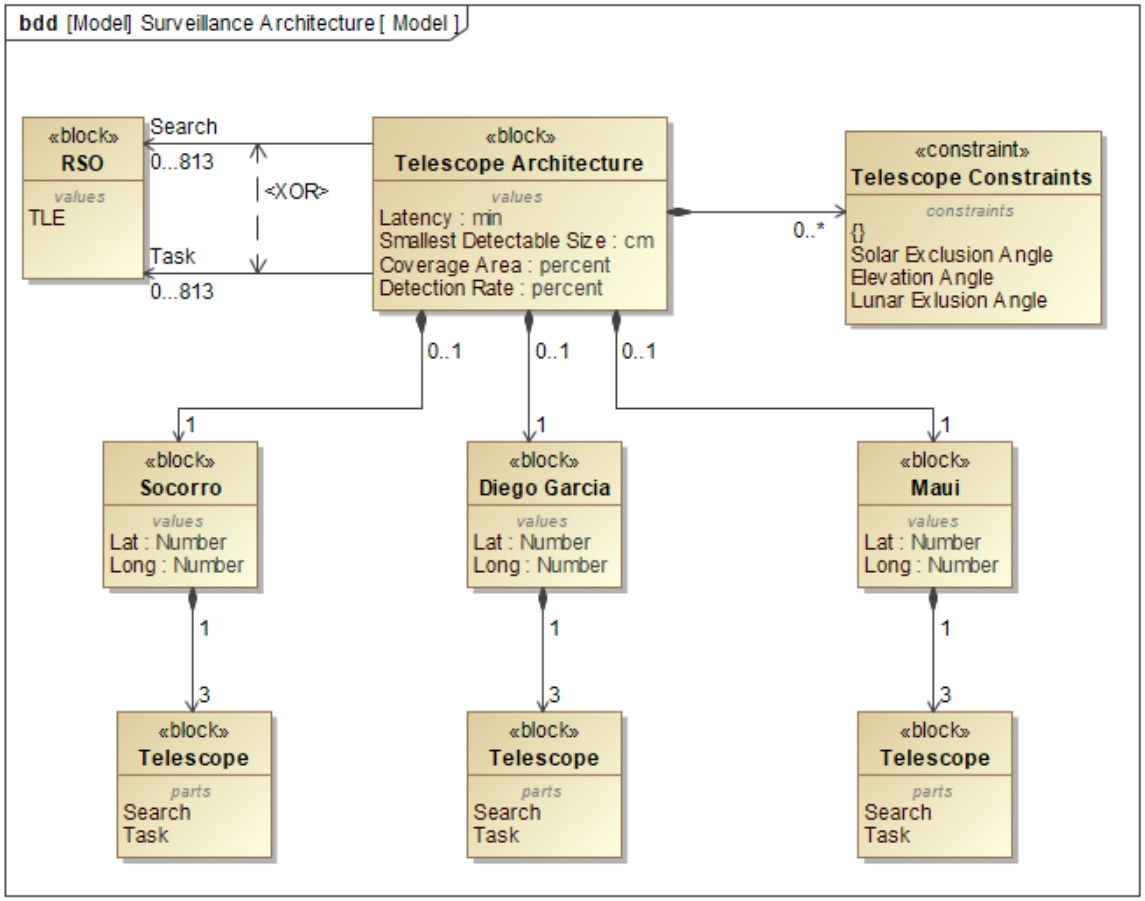

Fig. 4. Block Definition Diagram of the Model Architecture

Copyright © 2019 Advanced Maui Optical and Space Surveillance Technologies Conference (AMOS) – www.amostech.com

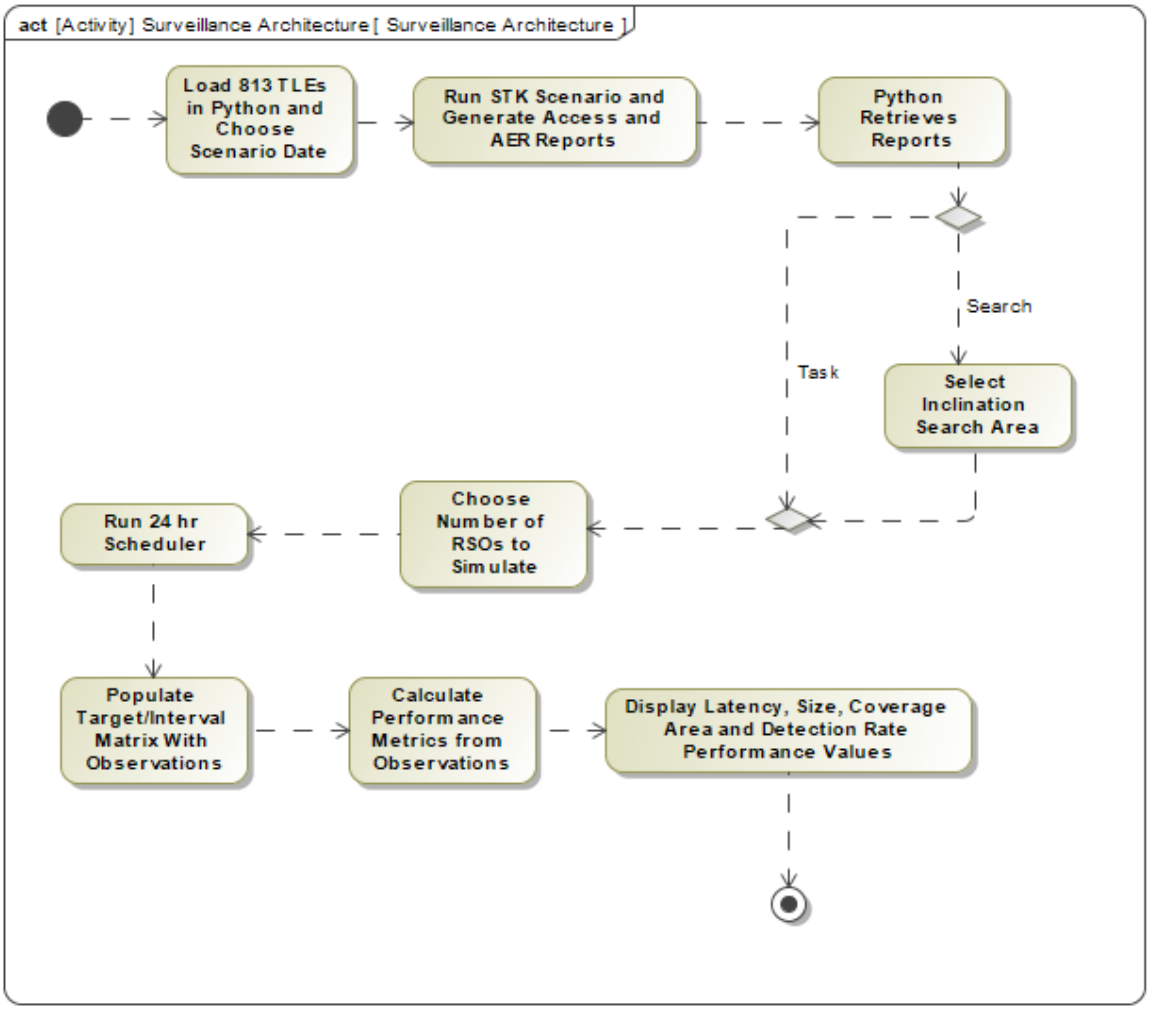

Fig. 5. Activity Diagram of Model

Data Generation

The first step in assessing performance is to create the scenario and generate the data needed for the scheduler. Using Python and connect commands with STK, the scenario was set up for a 24-hour period on the summer solstice, fall equinox, and winter solstice in 2018 with time steps of 30 seconds. The 21 Jun, 22 Sep, and 21 Dec dates were chosen to get results for the varying lighting conditions during the year. Ground-based telescopes were placed at the three locations: Socorro, NM; Maui, HI; and Diego Garcia. All telescopes were given solar exclusion angles of 40º, lunar exclusion angles of 10º, and minimum elevation angles of 15º; and they were limited to operating in umbra. Stern and Wachtel (2017) and Felten (2018) used 20º for minimum elevation. In "Analysis of a Simulated Optical GSO Survey," 10º elevation was used [7]. A 15º minimum elevation was used in this research to more closely model existing operations.

Simulated RSOs were generated using the 813 GEO TLES obtained from spacetrack.org. All RSOs were assigned the J2 perturbation model and were assumed to only be visible to the ground stations when they were in direct sunlight.

Once all RSO and ground stations were created, STK runs the scenario and generates lunar and solar phase angles, lunar and target zenith angles, access reports, azimuth/elevation/range reports, and moon phase reports for every ground station to RSO pair. These reports were then used in modeling the scheduler for both the task-based and search-based schedulers.

Since all data generated is in the local azimuth and elevation reference frame, a transformation formula was coded to convert from a local frame to a global latitude/longitude frame for each of the ground station locations. Transformation is necessary to figure out the telescope viewing limits to constrain the search pattern in the global

Copyright © 2019 Advanced Maui Optical and Space Surveillance Technologies Conference (AMOS) – www.amostech.com

reference frame. This longitudinal range is constrained by the minimum 15º elevation angle and the lowest altitude of the GEO belt, approximately 35,595 km, as viewed from the location of the ground station. As an example, due to Diego Garcia's location near the equator, it is able to see GEO RSOs in the entire range of +/- 16.97º declination from 10ºW to 135ºW longitude. Thus the search area for Diego Garcia telescopes is constrained to this coordinate box.

Scheduler

Baseline Task-Based Scheduler

A baseline model of current task-based operations is needed to create a comparison. The scheduler modeled by Stern and Wachtel was used to simulate the current task-based operations. The scheduler assumes it takes 30 seconds to take a 3-observation tracklet and then slew to the next RSO. A typical single observation exposure is 2–5 seconds. The Michigan Orbital Debris Survey used 5 seconds for exposures and the "Analysis of a Simulated Optical GSO Survey" technical paper used 2 seconds and 5 seconds for their models [7], [11]. Based on this, 30 seconds is a sufficient amount of time to simulate three 5-second exposures and slewing to the next RSO location. The scheduler prioritizes RSOs by always observing the RSO in its field of regard that has the largest time gap from its last observation. An observation is only credited on the RSO that had the highest time gap and not for any other RSO that may have been in the same FOV at the time. The scheduler produces a matrix of 1s and 0s for each 30-second interval indicating whether the ground station has a line of site for each RSO. This matrix then feeds into the evaluation phase. The model's goal is to emulate the typical operations of completing the nightly observation task list sent from the CSpOC. The task-based scheduler is run on 21 Jun, 22 Sep, and 21 Dec.

Search-Based Scheduler

The search-based scheduler was developed assuming the same 30-second allotment to complete three 5-second exposures and required slewing operations. The scheduler simulates a scan of the GEO belt +/- 16.97º above and below the equator similar to the +/- 17º used by Flohrer (2005). To cover at least +/- 15º of inclination, eight FOV intervals had to be used, which expanded the search area to +/- 16.97º. Six FOV intervals would only cover +/- 12.73º. The scan starts in the eastern sky and works its way west, moving downward and then eastward after a completed vertical scan, staying within the +/-16.97º boundary, similar to the Choi paper. Each 30 seconds, the telescopes slew to the next FOV and perform its three 5-second exposures. Each FOV has an area of 1.4º x 4.2º to simulate a coordinated effort of 3 telescopes at the ground station moving in unison. GEODSS telescopes have an advertised FOV of 2º square and each site has 3 telescopes [12]. Fig. 6 shows the concept of the scanning motion with each rectangle representing a 30-second observation. As the telescopes scan the sky, any RSO that is within the FOV at the given interval is credited with being observed.

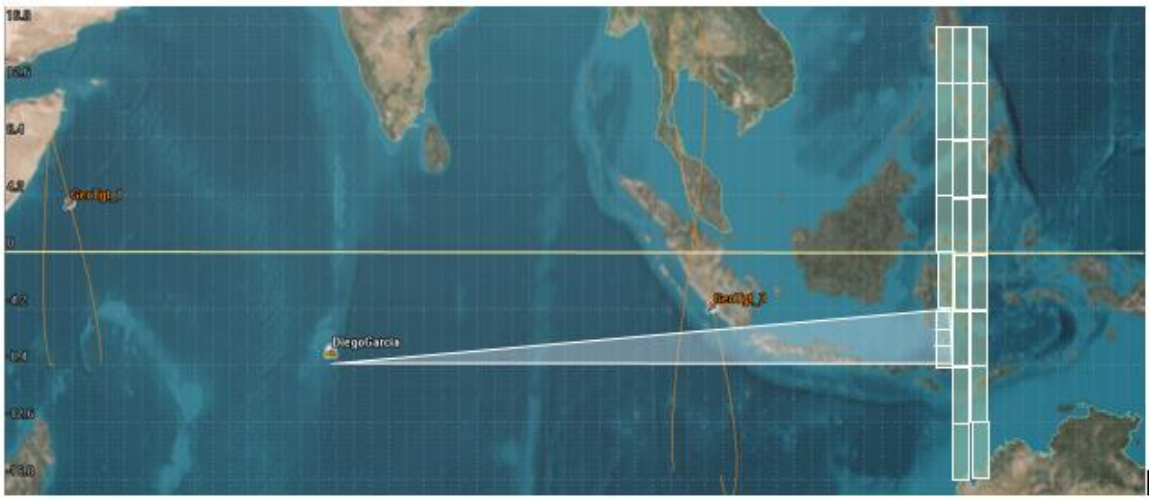

Fig. 6. Scanning Pattern of the Search-Based Scheduler

This scheduler produces a similar matrix of 1s and 0s as the task-based scheduler, indicating access at each interval for the ground station/RSO pair. This matrix also feeds into the evaluation phase. In addition to +/-16.97º, smaller

Copyright © 2019 Advanced Maui Optical and Space Surveillance Technologies Conference (AMOS) – www.amostech.com

searches of +/-12.73º, +/-8.48º, +/-4.24º, and +/-2.12º were run. The smaller search areas were a function of decreasing the number of latitudinal FOV intervals. The final run turned the FOV on its side, covering +/-0.71º in latitude and 4.24º in longitude. Each inclination search area was run on 21 Jun, 22 Sep, and 21 Dec, just like the tasking scheduler. Also, 10 different starting positions for each date and inclination search area were run. Search starting positions were equally spaced across each site's FOV. The first starting position starts in the eastern sky for each site location and then shifts west over to the next starting position. The 10 different starting positions provided more data points to make sure consistent values were being found for size, latency, and detection rate. Coverage area will remained constant because it is a function of the inclination search area.

Performance Evaluator

Minimum Detectable Size

For determining minimum detectable size, an assumed telescope performance of 18 visual magnitude was used instead of using an assumed SNR of 6, as used in the Stern and Wachtel (2017) and Felten (2018) theses. A visual magnitude of 18 is an approximate estimated performance of a 1-meter telescope. Equations (1–3) were used to solve for a minimum detectable size when given a visual magnitude [13].

$$F_{diff}(a_o, r_{sat}, \phi) = \frac{2}{3} \cdot a_o \cdot \frac{r_{sat}^2}{\pi R^2} \cdot (\sin(\phi) + (\pi - \phi)\cos(\phi)) \quad (1)$$

$$r_{sat} = \sqrt{\frac{RCS}{\pi}} \quad (2)$$

$$m_V(\phi) = -26.74 - 2.5 \cdot \log(F_{diff}(\phi)) \quad (3)$$

where,

F_{diff} is the incident solar flux reflected by the spherical RSO
a_o is the RSO's albedo
r_{sat} is the radius of the spherical satellite
R is the range between the RSO and the ground station
ϕ is the phase angle
RCS is the cross section of the RSO in square meters
m_V is the apparent visual magnitude.

It is assumed that the RSO is a Lambertian (diffusely-reflecting) sphere when using Equations (1–3) [13]. An albedo of 0.175 was used in this research and is consistent with Cognion's 0.2 and Stern and Wachtel's 0.15.

Atmospheric transmission is also factored in by using Laser Environmental Effects Definition Reference (LEEDR) to create an elevation vs. transmission curve. LEEDR was used to scale the drop in maximum visual magnitude performance from 90º elevation down to 15º. For nighttime viewing, objects lose about half their brightness going from 90º elevation to 15º, which equates to a loss of about one visual magnitude from the maximum viewable magnitude of the sensor [14]. For example, in this research, the maximum visual magnitude of 18 is at 90º and is scaled down as elevation approaches 15º, using the LEEDR atmospheric transmission curves. LEEDR curves were generated for each location and date. Equation (4) is used to calculate the reduced visual magnitude.

$$m_{V\,reduced} = 18 - (1 - \tau_{ATM}) \quad (4)$$

where,

τ_{ATM} is the atmospheric transmittance at a particular location, date and elevation angle.

The reduced visual magnitude is then used to solve for the radius of the satellite using Equations (1–3). Then diameter is calculated using Equation (5).

$$D_{min} = 2 * r_{sat} \quad (5)$$

Detection Rate

The second performance metric is detection rate, which is the number of RSOs that are observed out of the possible number of RSOs in the FOV of the network in a single 24-hour period. This is expressed as a percentage. Detection rate is calculated using Equation (6).

Copyright © 2019 Advanced Maui Optical and Space Surveillance Technologies Conference (AMOS) – www.amostech.com

$$DR = 100 * \frac{TO}{PT} \quad (6)$$

where,

DR is the detection rate percentage
TO is the number of unique targets observed
PT is the number of possible targets in the network FOV.[3]

Coverage Area

Coverage area is the third performance metric that is used to compare the task-based and search-based surveillance techniques. Coverage area is defined as the number of square degrees that were viewed, in the global reference frame, in a 24-hour period. Coverage area for the search-based technique is simply summing the area scanned by the three ground stations. Fig. 7 shows the three viewable regions of the GEO belt from each ground station location.

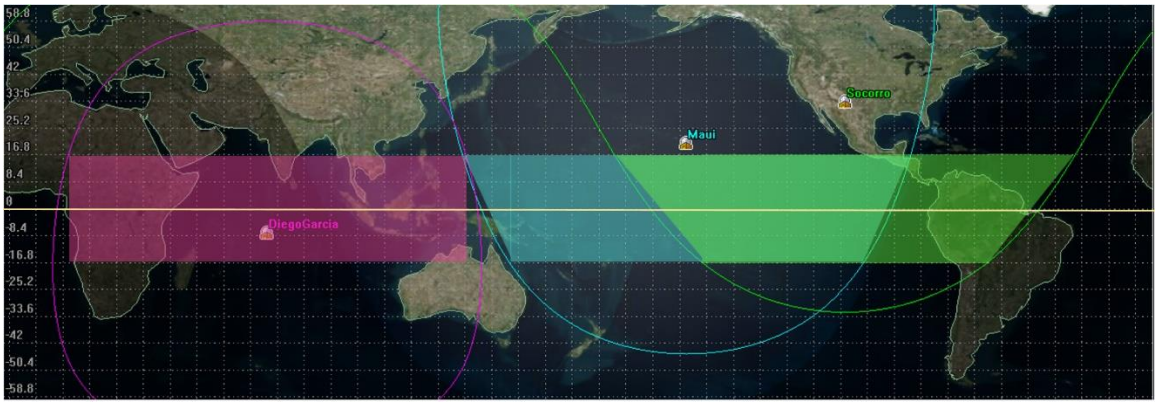

Fig. 7. GEO Belt Regions Viewable from Each Modeled Location

Coverage area for the task-based approach is more difficult to calculate. To come up with a coverage area provided by the task-based approach, a grid is set up with each box representing a 1.4ºx1.4º FOV. As the task-based scheduler runs, it takes observations of individual RSOs. When the observation is taken, the RSO is located in one of the 1.4ºx1.4º grid box FOVs. The task-based scheduler then gets credit for viewing that particular grid square of coverage area. As observations are taken through the night, the grid boxes are checked off as being viewed. At the end of the 24-hour period, the total number of squares viewed is summed up to give a total coverage area viewed by the task-based scheduler. Fig. 8 shows the concept of how coverage is tracked. Certain RSOs may be viewed multiple times along their orbit depending on the timing and access of the RSOs. Note that the grid is not to scale for viewing ease. Coverage area is calculated using Equation (7).

$$CA = 100 * \frac{VB}{TGB} \quad (7)$$

where,

CA is the coverage area percentage
VB is the number of 1.4ºx1.4º grid boxes viewed
TGB is the total number of 1.4ºx1.4º grid boxes within +/-16.97º of the equator.

[3] Network FOV is the total aggregated simulated FOV for all site locations.

Copyright © 2019 Advanced Maui Optical and Space Surveillance Technologies Conference (AMOS) – www.amostech.com

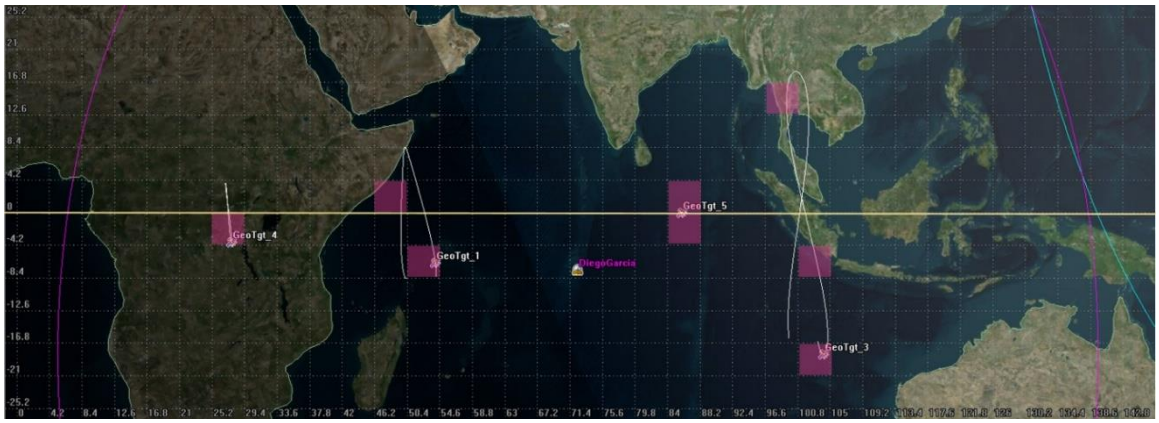

Fig. 8. Concept of Coverage Area Calculation for Task-Based Scheduler

Latency

The evaluator uses the interval/access matrix generated in the scheduler to produce the performance values for minimum detectable size and latency. Values were produced using the evaluation method similar to the Stern and Wachtel (2017) and Felten (2018) thesis. Their method produced a Mean of the Maximum Observation Time Gap (MMOTG) for latency. In this research, latency is simply the average of all time gaps for all RSOs. From Fig. 9, time gaps A–I are added to the rest of the 813 RSOs' time gaps and then averaged. RSOs that were unable to be viewed because of gaps in the simulated coverage were excluded from the calculation. Latency is calculated using Equation (8).

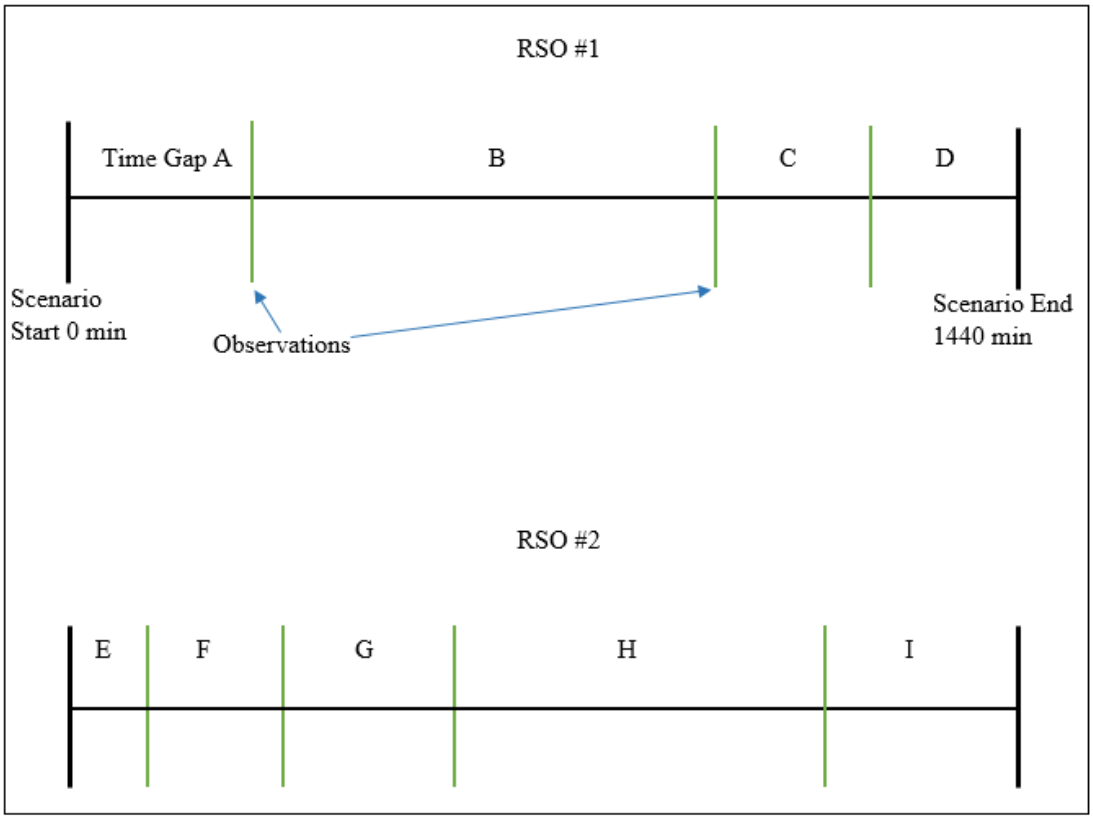

Fig. 9. Example of Time Gaps for Latency Calculation

Copyright © 2019 Advanced Maui Optical and Space Surveillance Technologies Conference (AMOS) – www.amostech.com

$$Latency\ (min) = \frac{\sum RSO\#1\ gaps + \sum RSO\#2\ gaps + \cdots \sum RSO\#n\ gaps}{Total\ Number\ of\ Time\ Gaps} \quad (8)$$

Assumptions

Two additional assumptions are made in the methodology. First, the percent cloud free line of site was 100%. Second, an object can be observed as long as it is in the FOV of the sensor at a particular time for the search method. No FOV edge effects were incorporated.

Results

Minimum Detectable Size

Minimum detectable size is the smallest size RSO the telescope would be able to detect—at the observed range, elevation angle, and solar phase angle—with a sensor capable of seeing objects as faint as 18 visual magnitude. Approximate size can be calculated for each observation by solving Equations (1–3) for the radius. The radius is then converted to a diameter. Table 1 shows the results for the average minimum detectable diameter for the various GEO belt inclination searches and time of year. As described in the methodology, six inclination searches were evaluated up to +/- 16.97º.

The results show that on average, the search method can see slightly smaller objects than the baseline tasking method. On each day, every type of inclination search produces a better size than the tasking method. The reason searching can see smaller objects could be that it better follows the anti-solar point[4] than the task-based approach. The tasking approach slews randomly around the GEO belt and may not obtain many observations at optimal phase angles. With search, several observations will be taken at or near the anti-solar point with each scan of the night sky.

Table 1. Minimum Average Detectable Size Diameter in Centimeters

	21 June 2018	22 Sep 2018	21 Dec 2018	Average
Baseline Tasking[5]	45.2	47.9	49.6	47.6
Search[6] +/- 16.97º	34.1	36.2	44.6	38.3
Search[6] +/- 12.73º	41.3	40.2	39.4	40.3
Search[6] +/- 8.48º	40.6	39.9	46.7	42.4
Search[6] +/- 4.24º	41.2	43.1	45.3	43.2
Search[6] +/- 2.12º	42.3	46.0	45.9	44.7
Search[7] +/- 0.71º	42.4	46.7	47.0	45.4
Average	40.3	42.0	44.8	

Another trend discovered was minimum detectable size was the best at the summer solstice and got worse as it went toward the winter solstice, even though atmospheric attenuation is higher in the summer. The average size across all methods for 21 Jun, 22 Sep, and 21 Dec was 40.3 cm, 42.0 cm, and 44.8 cm respectively. This trend is due to the locations of the simulated network of telescopes used. Two of the three telescopes are located at northern latitudes and the third is only a few degrees south of the equator. In the summer, the network has better solar phase angles during the night due to the tilt of the Earth and the majority of observations coming from northern latitude telescope locations.

[4] Anti-solar point is the point on the celestial sphere directly opposite the sun from an observer's perspective.
[5] Single telescopes with 1.4ºx1.4º FOV (Latitude x Longitude).
[6] Three telescopes with combined 4.2ºx1.4º FOV (Latitude x Longitude).
[7] Three telescopes with combined 1.4ºx4.2º FOV (Latitude x Longitude).

Copyright © 2019 Advanced Maui Optical and Space Surveillance Technologies Conference (AMOS) – www.amostech.com

A third trend is that the minimum detectable size is somewhat insensitive to the search areas utilized. Generally, minimum detectable size increases as the inclination search area decreases; however, at the +/- 8.48º search on 21 Jun and 22 Sep, and the +/- 12.73º and +/- 4.24º searches on 21 Dec, the minimum detectable size decreased.

The last trend identified was minimum detectable size generally gets larger as the inclination search area gets smaller. This shows that the best method to get the smallest overall minimum detectable size is to use the +/- 16.97º search pattern. A reason for this could again be that the +/- 16.97º search area follows the anti-solar point better than the other inclination searches. As the search area decreases, the rate at which the search progresses across the sky increases causing it to take more observations away from the optimal anti-solar point. In addition, starting in the eastern part of the sky each night gave the smallest average detectable size. Starting searches in the east allows the search to start closer to the anti-solar point, creating better phase angles resulting in smaller overall detectable size performance.

Detection Rate

Detection rate is the percent of RSOs that get at least one observation out of the total number of RSOs that are in the network FOV. Recall that 813 GEO RSOs are simulated, however only 722 RSOs on 21 Jun, 728 on 22 Sep, and 730 on 22 Dec are in the network FOV. Percentages are calculated on the number of viewable RSOs. Table 2 shows the results for detection rates with the different surveillance methods and time of year averaged over the ten different starting positions for each site. As an example, the search method with a +/- 16.97º search area on 21 June had an average detection rate of 96.4% over the ten starting locations. This excludes the RSOs that are in the network's coverage gap. Unlike the minimum detectable size, the detection rate does not appear to get better or worse with a western or eastern starting point.

Table 2. Detection Rates

	21 June 2018	22 Sep 2018	21 Dec 2018	Average
Baseline Tasking	100%	100%	100%	100%
Search +/- 16.97º	96.4%	96.7%	97.4%	96.8%
Search +/- 12.73º	96.4%	95.8%	97.8%	96.7%
Search +/- 8.48º	95.5%	94.0%	97.2%	95.6%
Search +/- 4.24º	95.0%	92.9%	97.0%	95.0%
Search +/- 2.12º	92.8%	91.7%	96.5%	93.7%
Search +/- 0.71º	90.1%	89.2%	95.7%	91.7%

The baseline tasking method observes 100% of the RSOs in the FOV due to the nature of the 30-second greedy scheduler and the assumption of a cloudless night. The tasking scheduler observes the RSO that has the longest unobserved time, therefore all RSOs in the network FOV eventually get one observation.

A noticeable trend is detection rate decreases as the inclination search area gets smaller. As seen in the rightmost column of Table 2, the average detection rate across the three dates is steady at the +/- 16.97º and +/- 12.73º searches but then begins to decline as the search area decreases Intuitively, this make sense; as inclination search area decreases, the chance of seeing higher inclined RSOs decreases. Fig. 10 shows the inclination distribution of the 813 RSOs used in the model. The bulk of the RSOs are below 16º. Although more passes are made across the sky as the search area decreases, which makes more opportunities for detections, it is not enough to keep the detection rate from dropping.

Copyright © 2019 Advanced Maui Optical and Space Surveillance Technologies Conference (AMOS) – www.amostech.com

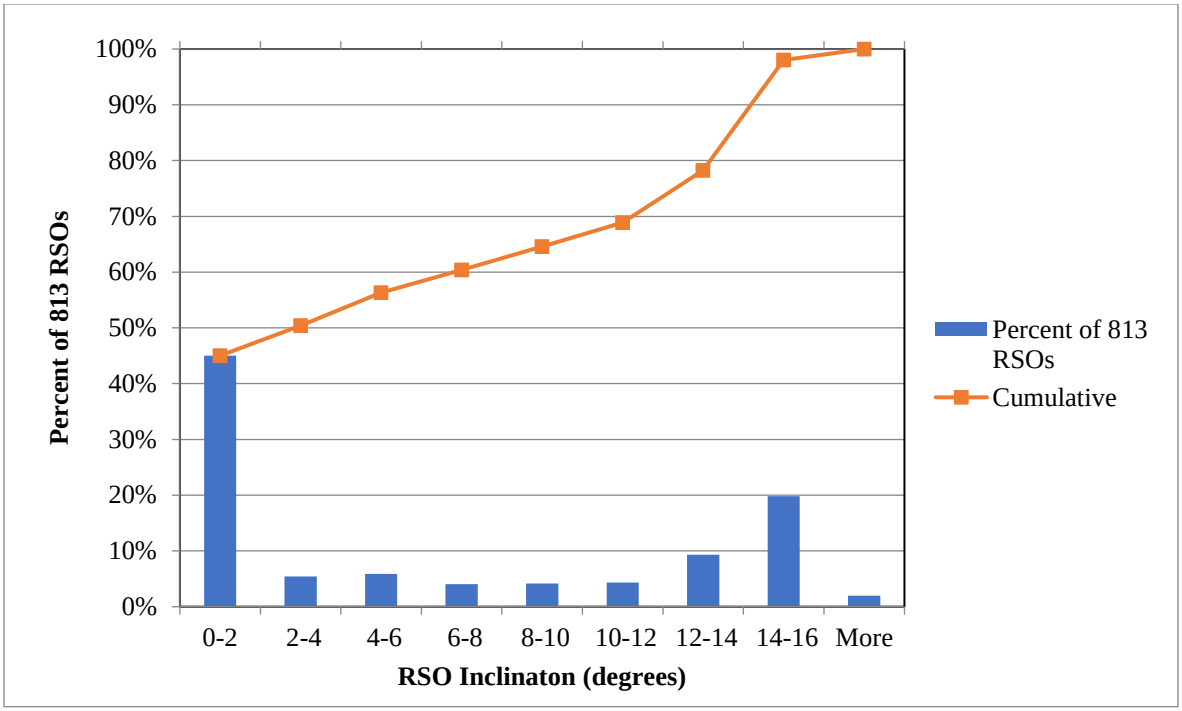

Fig. 10. Inclination Distribution of the 813 RSOs

Coverage Area

Coverage area is the amount of area between +/- 16.97º above and below the equator that is observed by the telescope as explained in the methodology. Fig. 11 shows the graph of the coverage area percent vs. the number of RSOs used in the scenario.

Copyright © 2019 Advanced Maui Optical and Space Surveillance Technologies Conference (AMOS) – www.amostech.com

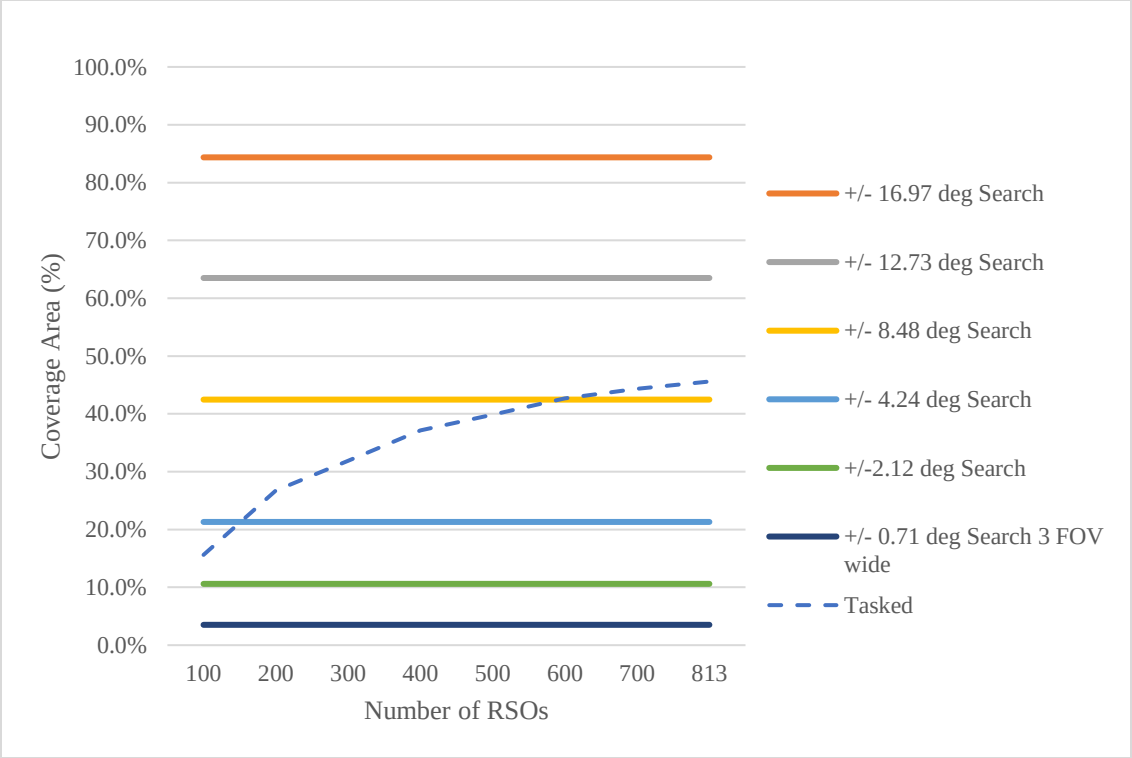

Fig. 11. Comparison of Tasked-Based Coverage vs. Different Search Methods

The graph shows that search coverage area does not change as the number of RSOs in the model are added. The search will cover the same amount of sky no matter how many RSOs are in the scenario. The search method has a max coverage of 84.4% at the +/- 16.97º search since the network has a coverage gap over the Atlantic Ocean. The gap can be seen on the right and left edges of Fig. 7. Coverage area obviously goes down as the inclination search area is narrowed. Tasking coverage area increases as more RSOs are added to the model, but it levels off at about 46%. The more RSOs that are available to observe, the more of the sky is viewed, which is reflected in the graph. However, this trend tapers off, as seen by the flattening of the task-based curve. This flattening is due to the inclinations of the 813 RSOs used. Recalling Fig. 10, the majority of RSOs have inclinations less than 6º. Most task-based observations will be made within 6º of the equatorial line. The task-based method has very few opportunities to view RSOs at higher inclined areas. Also, the coverage area did not change with respect to the time of year for either search or task mode. The search method has better coverage than the task method with the +/- 16.97º and +/- 12.73º searches but not at the smaller search areas.

However, when looking at the detection rate results in the previous section and considering that every RSO in GEO crosses the equatorial line, it is apparent that coverage area is not a good discriminator for performance unless searching "blank space" is important for SSA.[8] Even though coverage area is only 3.5% for the +/- 0.707º three wide search, the search strategy still acquires observations on about 92% of the possible RSOs in the network FOV. This shows that having the largest coverage area (84.4%) marginally improves detection rate (98.6%). A major drop in coverage area (3.5%) does not correlate to a major drop in detection rate (91.7%). The next section shows that a smaller search area does improve the latency.

Latency

Latency is simply the time between observations of a particular RSO. Table 3 shows the results for latency with the different surveillance methods and time of year averaged over the ten different starting positions for each site. Like the detection rate, latency does not appear to get better or worse with a western or eastern starting point. Several trends can be seen from the results.

[8] Finding new smaller objects will require searching "blank space."

Copyright © 2019 Advanced Maui Optical and Space Surveillance Technologies Conference (AMOS) – www.amostech.com

Table 3. Latency Results for Task and Search Methods in Minutes

	21 June 2018	22 Sep 2018	21 Dec 2018	Average
Baseline Tasking	84	78	72	78
Search +/- 16.97º	488	487	433	469
Search +/- 12.73º	428	428	371	409
Search +/- 8.48º	354	357	304	338
Search +/- 4.24º	239	237	204	227
Search +/- 2.12º	152	150	129	144
Search +/- 0.71º	65	65	55	62

The first trend is generally that as the nights get longer from June to Dec, the latency goes down. As mentioned earlier, due to the northern latitude location of two of the three telescope sites, longer observation times for the network happen in the winter. The longer nights allow for more observations to be made bringing down the overall latency.

The second trend is the overall latency improvements are greater from 22 Sep to 21 Dec than from 21 Jun to 22 Sep. The latency for the +/- 8.48º search actually increases from 21 June to 22 Sep. This increase in latency and difference in improvements is due to the 22 Sep date being in the middle of eclipse season. Eclipse season is when the Earth passes between the RSO and the sun from 26 Feb to 13 Apr and from 21 Aug to 15 Oct. This causes RSOs to be unviewable with optics during periods of the night.

The third and most obvious trend is latency improves as the search area is decreased. As the search area gets smaller, the telescopes can make more passes across the sky. More observations are made as the number of passes increases, thus lowering the overall latency. In this scenario with 813 RSOs, the search method outperforms the tasking method but only with the +/- 0.71º three FOVs wide search area.

The last two trends are shown in the latency results depicted in Fig. 12. The graph is the average latency over the three days vs. the number of RSOs in the scenario. The graph shows that search latency stays fairly constant for each inclination search area as the number of RSOs in the scenario increases, while the tasking latency increases linearly as number of RSOs increases. A linear fit to the tasking results gives the following Equation (9) for latency.

$$Tasked\ Latency\ (\text{min}) = 0.096544x + 0.8712 \quad (9)$$

where,

x is the number of RSOs in the scenario

Keep in mind the graph is the average latency of the easternmost starting positon and not an average over all ten starting positions.

Copyright © 2019 Advanced Maui Optical and Space Surveillance Technologies Conference (AMOS) – www.amostech.com

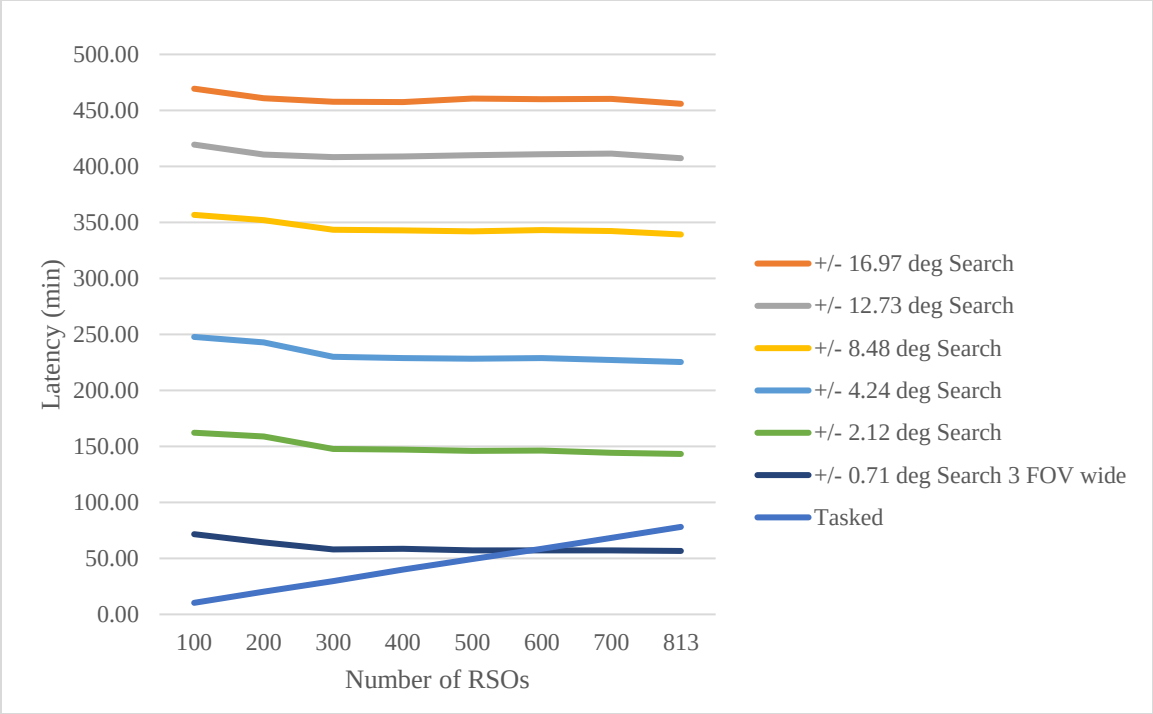

Fig. 12. Average Latency vs. Number of RSOs in a Scenario at the Eastern Starting Position

For each of the other search areas greater than the +/- 0.71º three FOVs wide method, the latency is greater than the tasking method. However, for each of these search areas, there is an approximate crossover point at which the tasking method will have longer latency than the search method. As an example, the +/- 4.24º inclination search area will be used to estimate the crossover point. Using the Equation (9) and a latency of 227 minutes, average latency for the +/- 4.24º search across the three dates, solve for the approximate number of RSOs that would be the crossover point for latency performance. The crossover point is 2,343 RSOs with the assumption that they have the same distribution in GEO as the 813 RSOs used. This means the task-based method performs better than the +/- 4.24º search method up to 2,343 RSOs in the scenario. Anything over this number, the search method has better latency performance. Table 4 presents the crossover number for each search method. Recall from the background section, NASA estimates there are more than 3,250 RSOs greater than 10 cm in diameter in GEO as of 2010 [6]. Using NASA's estimate for GEO population, the crossover point for latency performance would be close to the +/- 8.48º search area. Again, this is assuming the same distribution of orbital elements for the additional RSOs as the 813 RSOs used in this model. Actual RSO orbital element distributions would likely be different and produce different results.

Table 4. Latency Crossover Points Where Search-Based Method Will Outperform Task-Based

Search Area	+/-16.97º	+/-12.73º	+/-8.48º	+/-4.24º	+/-2.12º	+/-0.707º 3 wide
Number of RSOs	4,860	4,235	3,506	2,349	1,489	641

Latency is calculated by taking the average of all the time gaps. When taking an average, it is important to look at the distribution of the data. There was some concern that time gaps representing daytime gaps would dominate the distribution. For the task method, 93% of the time gaps were less than two hours while the time gaps that represented daytime, ten hours and greater, were at most 4% of the total time gaps. For the +/- 16.97º search method, daytime gaps represent 20–25% of the total time gaps. There is a visible increase in frequency at the 10–14 hour bins for the +/- 16.97º search method on the histogram graph. This representation decreases as the search areas get smaller and number of shorter time gaps increases due to the increased number of observations.

Copyright © 2019 Advanced Maui Optical and Space Surveillance Technologies Conference (AMOS) – www.amostech.com

Relevant Research Comparison

Recalling the background section, Choi found that the method for surveying had detection rates of 90% and 95% for non-operational and operational RSOs respectively. Choi used 287 RSOs over a single site located in South Korea and used an up and down scanning pattern within a +/-17º search area [7]. Flohrer's model used 4 locations placed around the world with 793 simulated RSOs. Flohrer simulated "strip" scanning, constraining the search area to +/-17º, and obtained detection rates of 89.8% and 94.7% for 8-hour and 12-hour observations per night respectively, similar to Choi's detection rates. Flohrer's research also determined objects could be seen down to 25 cm in diameter [8].

This research used a similar search pattern and search area as Choi and found similar detection rates ranging from 91.7% to 96.8%. It expanded the scope by using 813 RSOs with a network of three locations and multiple telescopes at each location. It found minimum detectable size averages of 38–48 cm in diameter. This research went beyond the previous researcher's results by adding ways to measure a search-based space surveillance method by calculating latency and coverage area.

Conclusion

New ways of ground-based telescope space surveillance operations can be modeled and assessed for performance. This research can provide answers on how to best utilize ground-based telescope networks. It can help provide insight into the advantages and disadvantages of new ways of performing space surveillance with ground-based telescopes without having to perform costly tests and take away from operational time. This research could also be applied to any network of ground-based telescopes that want to find ways to improve their surveillance performance.

A best value decision matrix was used to choose the best method based on minimum detectable size, detection rate, and latency. The best value matrix gave equal weights to each of the three performance metrics. Coverage area was not used in the best value matrix since it was not a good discriminator of performance. Value scores from 0 to 1 were given to each performance metric for the task-based and search-based methods. Minimum detectable size was given values on a linear scale from 10 cm to 100 cm with a value score of 1 for 10 cm or smaller and 0 for 100 cm and larger. Detection rate was given values on a liner scale from 75% to 100% with a value score of 1 for 100% and 0 for 75% and lower. Latency was given values on a linear scale from 30 minutes to 600 minutes with a value score of 1 for 30 minutes or less and a 0 for 600 minutes or more. Table 5 shows that the task-based method has the highest overall value when performance is equally weighted.

Table 5. Best Value Results

	Size (cm)	Size Value	Detection Rate	Detection Value	Latency (min)	Latency Value	Value
Baseline Tasking	47.6	0.583	100.0%	1.000	78	0.912	0.832
Search +/- 16.97º	38.3	0.686	96.8%	0.872	469	0.208	0.589
Search +/- 12.73º	40.3	0.664	96.7%	0.868	409	0.316	0.616
Search +/- 8.48º	42.4	0.640	95.6%	0.824	338	0.444	0.636
Search +/- 4.24º	43.2	0.632	95.0%	0.800	227	0.644	0.692
Search +/- 2.12º	44.7	0.615	93.7%	0.748	144	0.793	0.719
Search +/- 0.71º	45.4	0.607	91.7%	0.668	62	0.941	0.739

However, at some point, there will be too many objects for the tasking method to outperform a search-based method in latency and detection rate. As seen from the background section, the number of objects in GEO has been increasing at a rate of two additions to one removal every year from 2000 to 2009 and there are over 3,250 objects in GEO greater than 10 cm as of 2010 [6]. In the future, if the GEO catalog expands to a few thousand objects, then either more telescopes would have to be built or a searching or scanning technique would be needed. If the catalog expanded to approximately 10,000 RSOs or more in GEO, depending on the time of year and distribution of added RSOs, the tasked-based method would not have enough time to make an observation on every RSO in a single night, which would cause a decline in detection rate.

On the other hand, switching to a 100% search method may not be the full answer to providing the best ground-based space surveillance. The ultimate goal of SSA is to know where everything is at all times. No search method

Copyright © 2019 Advanced Maui Optical and Space Surveillance Technologies Conference (AMOS) – www.amostech.com

was able to detect 100% of the possible objects each night. Choosing the largest inclination search area does produce a detection rate close to 97% and has the best minimum size detection, but it also has the worst latency performance of any method. Shrinking the inclination search area would decrease latency but would also decrease the detection rate.

It is very possible that a combination of task-based and search-based surveillance could be used to get the best performance. The smallest inclination search area could be used for the first portion of the night with a follow up of taskings that could get observations on RSOs that were missed during the search.

Bibliography

[1] J. P. 3-14 S. JP 3-14, "Joint Publication 3-14 Space Operations," no. April, 2018.

[2] M. Pomerleau, "DoD needs to know what's happening in space, general says," *Defense News*. [Online]. Available: https://www.defensenews.com/c2-comms/satellites/2018/06/22/dod-needs-to-know-whats-happening-in-space-general-says/.

[3] M. Gruss, "Russian Luch Satellite Relocates — Next to Another Intelsat Craft," *SACENEWS*. [Online]. Available: https://spacenews.com/russian-luch-satellite-relocates-next-to-another-intelsat-craft/.

[4] D. R. Coats, "WORLDWIDE THREAT ASSESSMENT of the US INTELLIGENCE COMMUNITY," 2018.

[5] B. Beyer and N. Nelson, "Space Congestion Threatens to 'Darken Skies,'" *National Defense*, Jun-2018.

[6] N. L. Johnson, "Orbital debris: The growing threat to space operations," *NASA Sp. Debris Q.*, 2010.

[7] J. Choi *et al.*, "Analysis of a Simulated Optical GSO Survey Observation for the Effective Maintenance of the Catalogued Satellites and the Orbit Determination Strategy," *J. Astron. Sp. Sci.*, vol. 32, no. 3, pp. 237–245, 2015.

[8] T. Flohrer, T. Schildknecht, R. Musci, and E. Stöveken, "Performance estimation for GEO space surveillance," *Adv. Sp. Res.*, vol. 35, no. 7, pp. 1226–1235, 2005.

[9] H. Krag *et al.*, "Proof - The extension of ESA's master model to predict debris detections," *Acta Astronaut.*, vol. 47, no. Nos. 2-9, pp. 687–697, 2000.

[10] T. Flohrer, T. Schildknecht, and R. Musci, "Proposed strategies for optical observations in a future European Space Surveillance network," *Adv. Sp. Res.*, vol. 41, no. 7, pp. 1010–1021, 2008.

[11] K. J. Abercrombly, P. Seitzer, E. S. Barker, H. M. Cowardin, and M. J. Matney, "Michigan Orbital DEbris Survey Telescope Observations of the Geosynchronous Orbital Debris Environment.," *NASA Sp. Debris Q.*, no. September, pp. 2007–2009, 2010.

[12] R. F. Bruck and R. H. Copley, "GEODSS present configuration and potential," *Adv. Maui Opt. Sp. Surveill. Technol. Conf.*, 2014.

[13] R. L. Cognion, "Observations and Modeling of GEO Satellites at Large Phase Angles," in *Proceedings from Advanced Maui Optical and Space Surveillance Technologies Conference*, 2013.

[14] B. Schaefer, "Atmospheric Extinction Effects on Stellar Alignmnets," *Archaeoastronomy*, vol. 10, no. xvii, pp. S32–S42, 1986.

Copyright © 2019 Advanced Maui Optical and Space Surveillance Technologies Conference (AMOS) – www.amostech.com